



# Engineered MoSe<sub>2</sub>/WSe<sub>2</sub> based heterostructures for efficient hydrogen evolution reaction

Rahul <sup>a,\*</sup>, Harpreet Singh <sup>a</sup>, N.P. Lalla <sup>b</sup>, Uday Deshpande <sup>b</sup>, Sunil Kumar Arora <sup>a</sup>

<sup>a</sup> Centre for Nanoscience and Nanotechnology, Sector-25, Panjab University, Chandigarh 160014, India

<sup>b</sup> UGC-DAE Consortium for Scientific Research, University Campus, Khandwa Road, Indore 452001, India

## ARTICLE INFO

### Article history:

Available online 16 February 2021

### Keywords:

Transition metal dichalcogenides

Liquid exfoliation

Hydrogen evolution reaction

Electrocatalyst

## ABSTRACT

Electrocatalytic water splitting into hydrogen and oxygen using semiconducting heterogeneous nanostructures is a promising and emerging technology. Semiconductor materials based heterogeneous nanostructures have attracted much attention to be used as catalysts, co-catalysts, photocatalysts and photo absorbers. The present work deals with the investigation of heterostructures of molybdenum selenide (MoSe<sub>2</sub>) and tungsten selenide (WSe<sub>2</sub>) nanosheets prepared through liquid exfoliation method as electrocatalysts for the hydrogen evolution reaction (HER). Our experimental studies reveal that MoSe<sub>2</sub>/WSe<sub>2</sub> heterostructures synthesized using hydrogen peroxide (H<sub>2</sub>O<sub>2</sub>) exhibits superior HER performance. These novel structures leads to the exposure of more catalytically active sites and maintains effective electron transport, resulting in a small Tafel slope of 80 mV/decade and large electrochemical surface area (ECSA) of 87. This low-cost method finds application in high-performance HER electrocatalyst.

© 2021 Elsevier Ltd. All rights reserved.

Second International Conference on Aspects of Materials Science and Engineering (ICAMSE 2021).

## 1. Introduction

There is a global quest to shift to renewable sources of energy as the traditional fossil fuels are rapidly diminishing and are hazardous to the environment. The ultra-high energy density of hydrogen makes it one of the most reliable and eco-friendly energy source. In order to produce very pure hydrogen, hydrogen evolution reaction (HER) is employed. However, the choice of costly and scarcely available platinum group metals as electrocatalyst for HER has hampered the large-scale hydrogen production. Recently, two-dimensional (2D) transition metal dichalcogenides (TMDs) have garnered huge attention owing to their abundance and unique electrocatalytic activity towards the hydrogen evolution reaction (HER) [1,2].

Usually, TMDs are prepared either by top/down micromechanical cleavage or bottom-up chemical-vapor deposition (CVD) [3,4]. These methods are suitable only for producing either single or few-layer nanosheets. For applications which do not require stringent thickness control, the transition metal dichalcogenide (TMD) nanosheets synthesized by liquid exfoliation [5] and Li-intercalation methods [6] can be used.

To optimize the HER catalytic activities using TMDs, different approaches have been followed to synthesize TMD nanostructures

with a high density of active edge sites [7,8]. Some of the methodologies to proliferate active edge site density include creation of vertically aligned layers of TMDs [9], controllable disorder in ultra-thin molybdenum sulphide (MoS<sub>2</sub>) nanosheets with oxygen incorporation [10], porous exfoliated molybdenum selenide (MoSe<sub>2</sub>) suspensions [11] and unique vertically standing stack structure of MoS<sub>2</sub> nanosheets [12]. These studies evidently demonstrate that the increasing active sites play a vital role in attaining greater HER activity. Furthermore the TMD heterostructures are reported to exhibit better electrocatalytic performance than their constituent counterparts [13]. This motivates us to examine ultra-thin and porous heterostructure of TMDs nanosheets with abundant active edge sites in order to design better HER catalyst rather than using traditional platinum (Pt) noble metal catalysts. In the present work, we aim at fabricating heterostructures of hydrogen peroxide (H<sub>2</sub>O<sub>2</sub>) treated molybdenum selenide (MoSe<sub>2</sub>) nanosheets and tungsten selenide (WSe<sub>2</sub>) nanosheets through liquid exfoliation method and their subsequent utilization as electrocatalysts for the HER.

## 2. Materials and methods

The Molybdenum selenide (MoSe<sub>2</sub>) (99.98%), Tungsten selenide (WSe<sub>2</sub>) (99.98%), and Nafion (5 wt%) were obtained from Alfa Aesar while Isopropanol (IPA) and hydrogen peroxide (H<sub>2</sub>O<sub>2</sub>) (30 wt%)

\* Corresponding author.

E-mail address: [rahulguleria863@gmail.com](mailto:rahulguleria863@gmail.com) (Rahul).

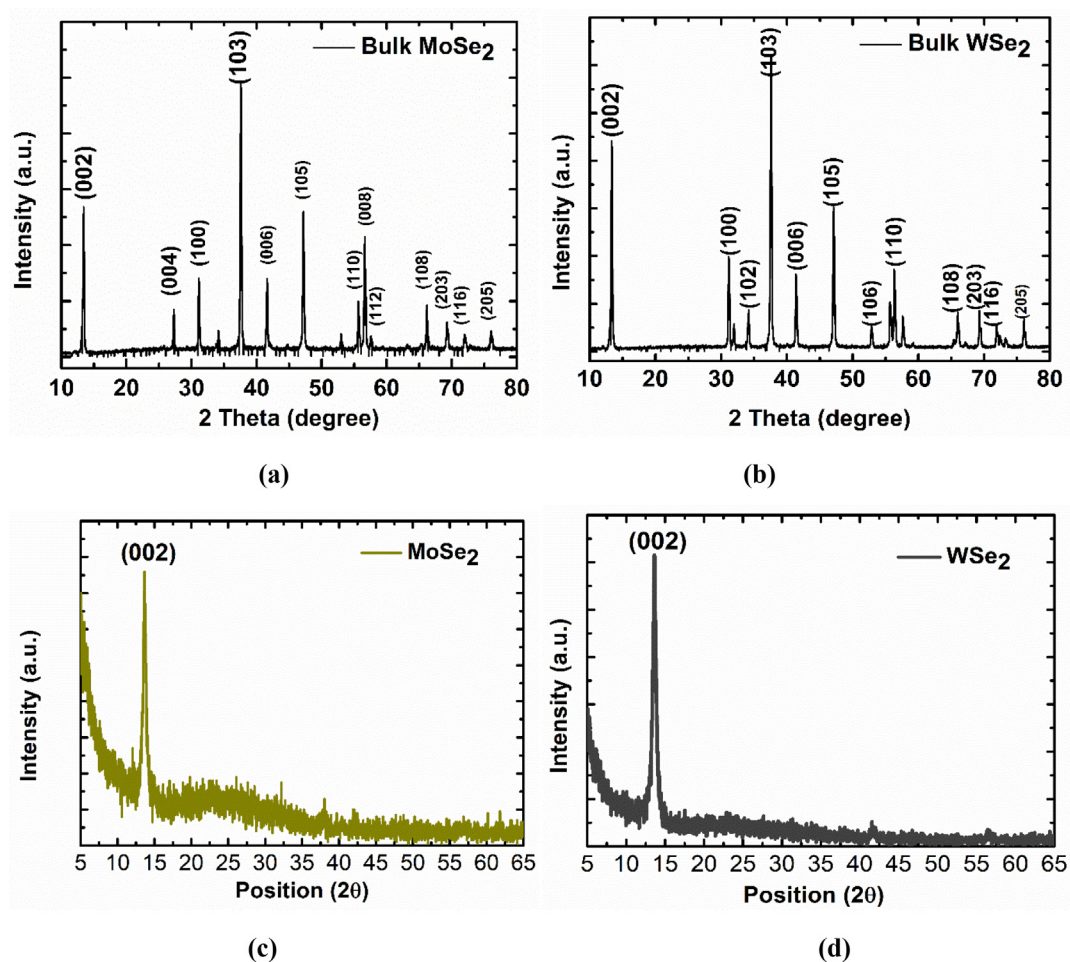


Fig. 1. XRD analysis of (a) bulk MoSe<sub>2</sub>, (b) bulk WSe<sub>2</sub>, (c) exfoliated MoSe<sub>2</sub> and (d) exfoliated WSe<sub>2</sub>.

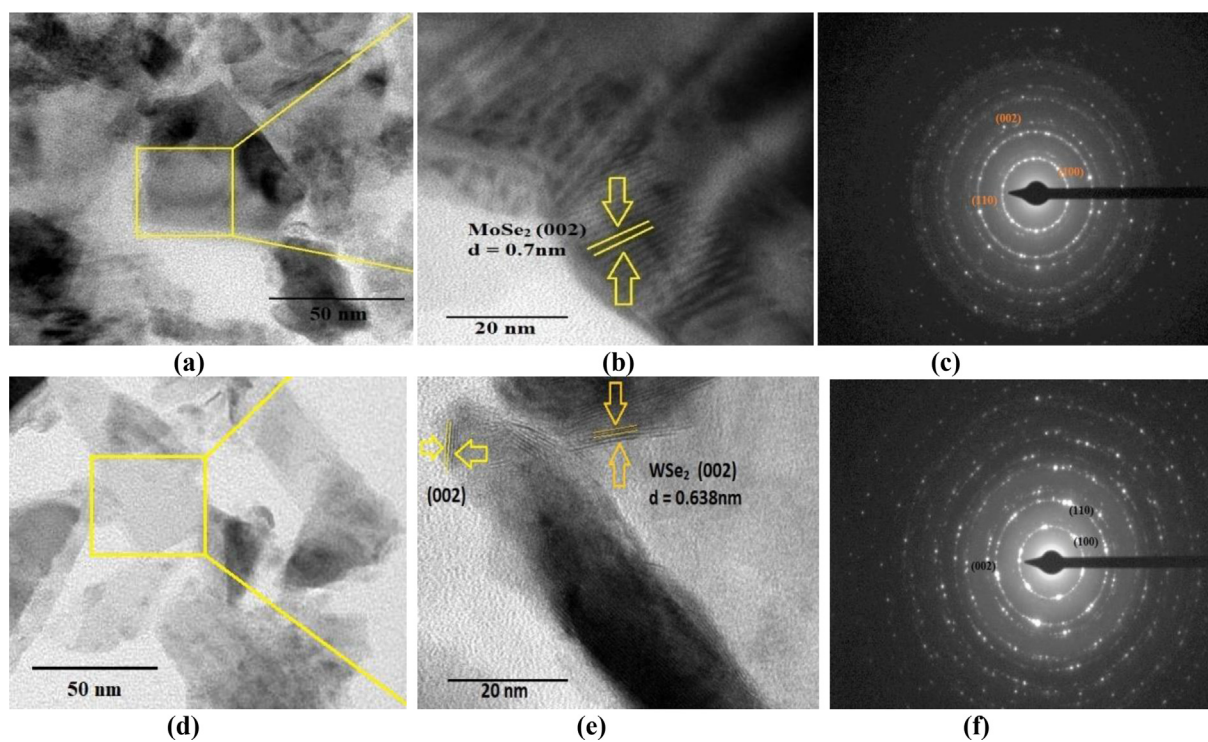
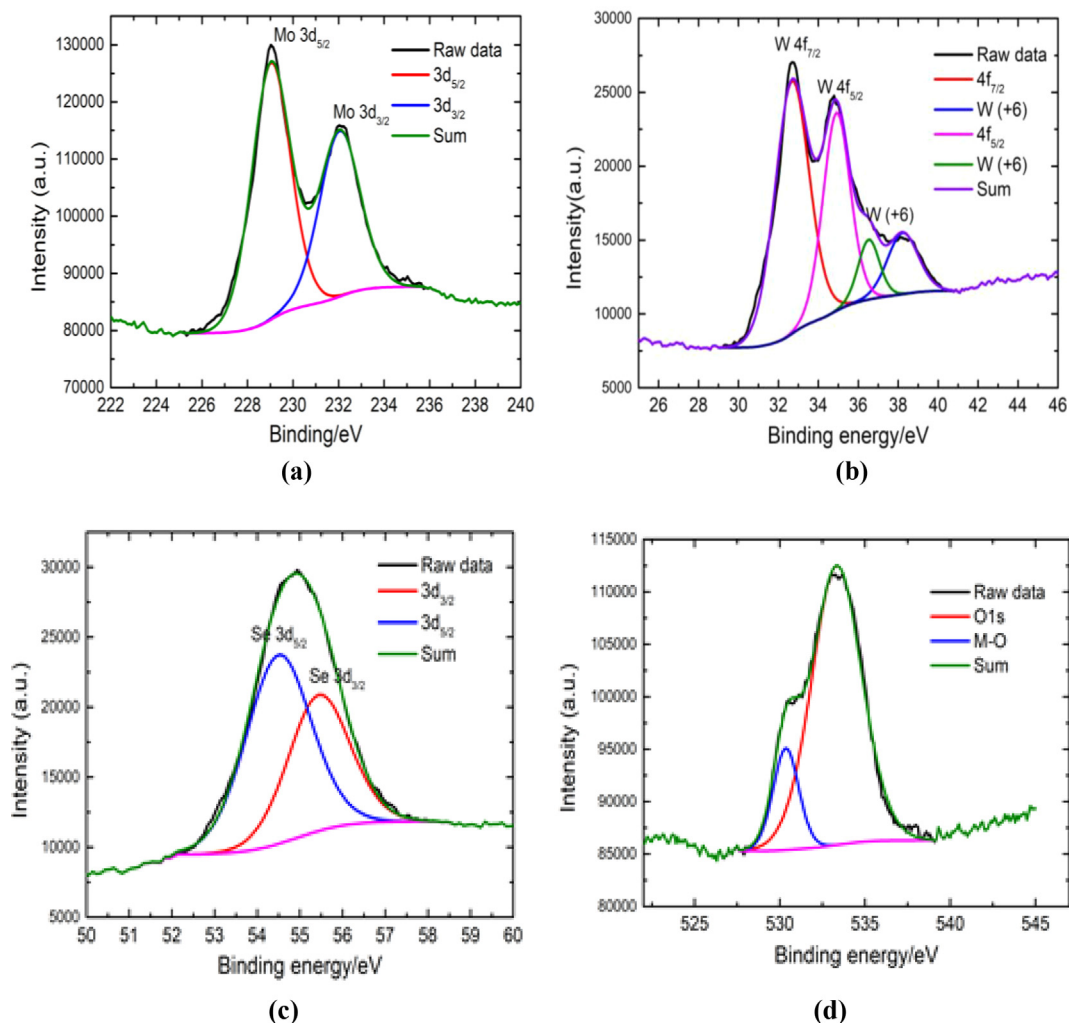


Fig. 2. The low and high magnification TEM images of (a, b) MoSe<sub>2</sub> and (d, e) WSe<sub>2</sub> respectively. (c) and (f) shows the corresponding SAED pattern of MoSe<sub>2</sub> and WSe<sub>2</sub>.



**Fig. 3.** High-resolution XPS spectra and corresponding deconvoluted spectra of (a) Mo 3d of MoSe<sub>2</sub>, (b) W 4f WSe<sub>2</sub> and (c) Se 3d; (d) O 1 s core-level and corresponding deconvoluted spectra of the O1s.

were procured from Sigma–Aldrich. All the reagents were of analytical grade and used without further purification.

To prepare MoSe<sub>2</sub> and WSe<sub>2</sub> nanosheets using liquid exfoliation method, 1 g each of MoSe<sub>2</sub> and WSe<sub>2</sub> were dispersed in a flask containing 100 mL of IPA. The sealed flasks having MoSe<sub>2</sub> (WSe<sub>2</sub>) were then sonicated for 4hrs (5hrs) and subsequently left to settle down for 12 hrs. Thus, obtained supernatant solutions were centrifuged at 3000 rpm for 40 min in order to get few monolayer (ML) thick nanosheets.

To synthesize porous MoSe<sub>2</sub>, it was exfoliated using IPA in the presence of 2.5 vol% of H<sub>2</sub>O<sub>2</sub>. For the purpose of preparing heterostructures, this solution was mixed with the dispersion containing WSe<sub>2</sub> nanosheets in 1:1 proportion. At last these suspensions were dried at 50 °C in vacuum to obtain the powder samples.

The X-ray diffraction (XRD) measurements were performed using Panalytical's X'pert Pro diffractometer using Cu-K $\alpha$  radiation ( $\lambda = 0.154$  nm) and the patterns were recorded from 20 to 80° in 2 $\theta$ . Electrochemical measurements were obtained with a computer-controlled potentiostat in a standard three-electrode cell using a platinum wire as a counter electrode and Silver/Silver Chloride (Ag/AgCl) (in 3 M Potassium Chloride (KCl) solution) as a reference electrode. To prepare the working electrode, 1 mg of sample was first ultrasonically dispersed in 300  $\mu$ L of Nafion solution (5 wt%), then  $\sim$ 10  $\mu$ L suspension was spread onto a glassy carbon (GC) electrode as a working electrode. For comparison,

working electrode of the few-layer H<sub>2</sub>O<sub>2</sub> treated and non-H<sub>2</sub>O<sub>2</sub> treated MoSe<sub>2</sub>, WSe<sub>2</sub> nanosheets and their heterostructure were prepared and measured. CV (cyclic voltammetry) curves were obtained on a potential range of 0.15–0.25 V vs Reversible hydrogen electrode (RHE) as reported before [14].

### 3. Results and discussions

Fig. 1 shows the X-ray powder diffraction (XRD) spectra corresponding to the crystal structures of TMDs nanosheets. Clearly Fig. 1(a–b) shows that the bulk MoSe<sub>2</sub> and WSe<sub>2</sub> were polycrystalline in nature and possesses hexagonal phase. Upon exfoliation the nanosheets exhibits unidirectional growth along (002) plane however (002) peak is broadened as compare to its bulk counterparts which visibly demonstrates the formation of few ML nanosheets.

The crystal structure of MoSe<sub>2</sub> and WSe<sub>2</sub> were further investigated by using Transmission electron microscopy (TEM). Fig. 2 (a–f) shows that the sample is flaky and shows crystalline diffraction. It is observed that the lattice fringes were separated by 0.7 nm (0.638 nm) for (002) crystal plane of MoSe<sub>2</sub> (WSe<sub>2</sub>). Further the crystalline nature of hexagonal MoSe<sub>2</sub> and WSe<sub>2</sub> structure were confirmed by the sharp diffraction spots in the selected area electron diffraction (SAED) measurements.



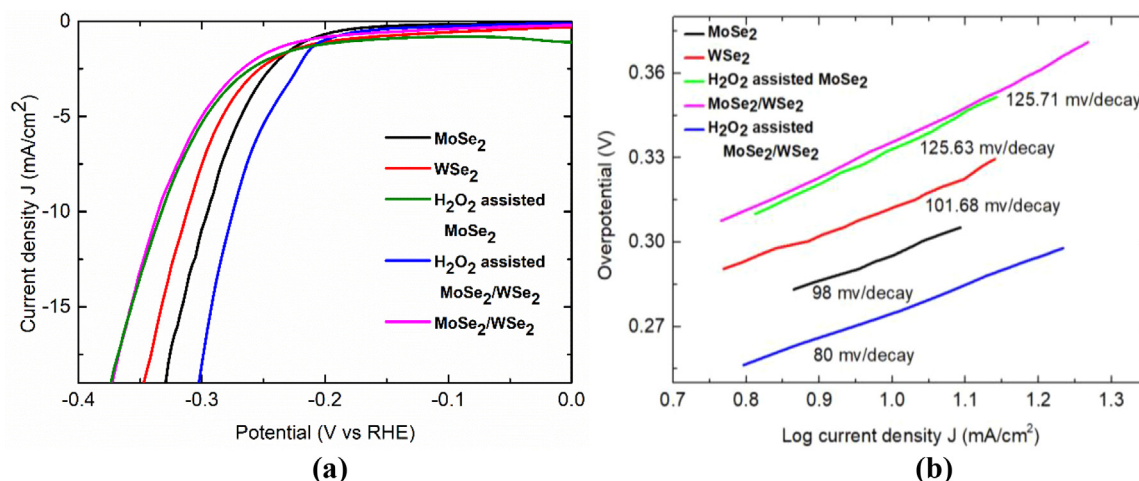


**Fig. 4.** (a) Correspond to the polarization curve of few-ML MoSe<sub>2</sub>, WSe<sub>2</sub>, H<sub>2</sub>O<sub>2</sub> treated MoSe<sub>2</sub> nanosheets, heterostructures of H<sub>2</sub>O<sub>2</sub> treated MoSe<sub>2</sub> and WSe<sub>2</sub> nanosheets, heterostructure of MoSe<sub>2</sub> / WSe<sub>2</sub> nanosheets and (b) correspond to their Tafel slope.

Fig. 3 shows the Mo 3d, W 4f, Se 3d and O 1s x-ray photoelectron spectroscopy (XPS) spectra of exfoliated MoSe<sub>2</sub> and WSe<sub>2</sub> nanosheets. In Fig. 3a the peaks located at binding energies of 229.1 (Mo<sup>4+</sup> 3d<sub>5/2</sub>) and 232.2 eV (Mo<sup>4+</sup> 3d<sub>3/2</sub>) are consistent with Mo(IV) oxidation state. The Se 3d core level spectra exhibit doublet peaks at 55.3 and 54.5 eV, which can be attributed to Se 3d<sub>3/2</sub> and Se 3d<sub>5/2</sub> of Se<sup>2-</sup> respectively. Furthermore, the W 4f<sub>7/2</sub> and W 4f<sub>5/2</sub> peaks located at 32.1 and 34.2 eV respectively, which corresponds to the +4 oxidation state of W. Also, the additional peak at 37.9 and 35.7 eV were obtained upon deconvolution. The observed peaks can be assigned to W 4f<sub>7/2</sub> and W 4f<sub>5/2</sub>, which ascribe the presence

of +6 oxidation state of W. For both the WSe<sub>2</sub> and MoSe<sub>2</sub> the ~1:2 ratio obtained from integrated peak areas indicates the desired stoichiometry of prepared nanosheets.

Next, we will explore the potential of using heterostructures of MoSe<sub>2</sub>/WSe<sub>2</sub> nanosheets and H<sub>2</sub>O<sub>2</sub> treated MoSe<sub>2</sub>/WSe<sub>2</sub> nanosheets as electrocatalysts for HER. The HER activity was measured using the standard three electrode electrochemical configurations in 0.5 M H<sub>2</sub>SO<sub>4</sub> electrolyte (Fig. 4a). In addition to the above mentioned heterostructures, the HER activities of few-layer MoSe<sub>2</sub>, WSe<sub>2</sub> and their heterostructures were also evaluated for comparison purpose.

From Fig. 4, the calculated values of overpotential corresponding to the heterostructures of H<sub>2</sub>O<sub>2</sub> treated

MoSe<sub>2</sub>/WSe<sub>2</sub> nanosheets, exfoliated MoSe<sub>2</sub>, WSe<sub>2</sub>, MoSe<sub>2</sub>/WSe<sub>2</sub> heterostructures and H<sub>2</sub>O<sub>2</sub> treated MoSe<sub>2</sub> are 275.84 mV, 291 mV, 310 mV, 337 mV, 331 mV respectively. These numerical values clearly manifest that the heterostructures of H<sub>2</sub>O<sub>2</sub> treated MoSe<sub>2</sub> and WSe<sub>2</sub> nanosheets provide better HER activity than the few-layer MoSe<sub>2</sub>, WSe<sub>2</sub> nanosheets and their heterostructures. For further assessment of the electrocatalytic performance of a catalyst towards HER, Tafel slope derived from Tafel plots ( $Z = b \log j + a$ , where  $j$  is the current density and  $b$  is the Tafel slope) was computed as shown in Fig. 4b. Clearly the Tafel slope of the heterostructures of H<sub>2</sub>O<sub>2</sub> treated

MoSe<sub>2</sub>/WSe<sub>2</sub> nanosheets is minimum (80 mV/decade) making it the most suitable candidate as electro catalyst for HER.

Further to evaluate the effective electrochemical surfaces of the catalysts, the electrochemical double-layer capacitance ( $C_{dl}$ ) was measured [18]. Electric double-layer capacitance is based on the charge separation occurring at an electrode–electrolyte interface when voltage is applied, where electric charges are accumulated on the electrode surfaces while ions of opposite charge gather on

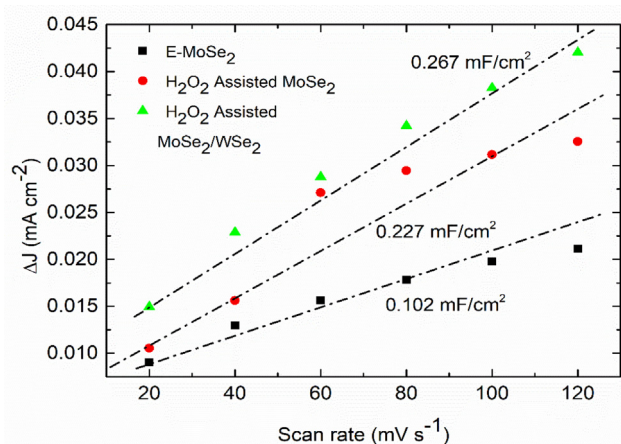


**Fig. 5.** Double layer capacitance slope of exfoliated MoSe<sub>2</sub>, H<sub>2</sub>O<sub>2</sub> treated MoSe<sub>2</sub> and heterostructure of few layer H<sub>2</sub>O<sub>2</sub> treated MoSe<sub>2</sub> WSe<sub>2</sub> nanosheets (at 300 K).

**Table 1**

HER performance parameters obtained from various structures.

Catalyst	Structure	Electrolyte	Overpotential 10 mA cm <sup>-2</sup>	Tafel mV/decade	ECSA	Reference
WSe <sub>2</sub>	Nanotubes	1 M H <sub>2</sub> SO <sub>4</sub>	365	99	—	[15]
Zn MoSe <sub>2</sub>	Nanosheets	0.5 M H <sub>2</sub> SO <sub>4</sub>	231	58	—	[1]
RH MoSe <sub>2</sub>	Nanoflower	0.5 M H <sub>2</sub> SO <sub>4</sub>	73	118	264	[16]
Porous MoSe <sub>2</sub>	Nanosheets	0.5 M H <sub>2</sub> SO <sub>4</sub>	150	80	79	[11]
MoS <sub>2</sub> /WS <sub>2</sub>	Thin films	0.5 M H <sub>2</sub> SO <sub>4</sub>	129	72	—	[17]
MoSe <sub>2</sub> /MoS <sub>2</sub>	Nanosheets	0.5 M H <sub>2</sub> SO <sub>4</sub>	162	61	—	[12]
H <sub>2</sub> O <sub>2</sub> assisted MoSe <sub>2</sub> /WSe <sub>2</sub>	Nanosheets	0.5 M H <sub>2</sub> SO <sub>4</sub>	275	80	87	This work

the electrolyte side. Double-layer capacitance was calculated by taking cyclic voltammetry (CV) curves at different scan rates of 20, 40, 60, 80, 100, 120 mV/s and eventually measuring the slope of the graph between the scan rate and difference in current density (at 0.38 V). Furthermore, specific capacitance was evaluated by performing CV at 50 mV/s. It is apparent from Fig. 5, that the heterostructures of H<sub>2</sub>O<sub>2</sub> treated MoSe<sub>2</sub>/WSe<sub>2</sub> nanosheets have the largest C<sub>dl</sub> of 0.267 mF/cm<sup>2</sup> and Electrochemical surface area (ECSA) of 87. Clearly our calculated values of C<sub>dl</sub> and ECSA are comparable to the priorly reported results as tabulated in Table 1.

#### 4. Conclusion

In summary, simple liquid exfoliation method was employed to prepare MoSe<sub>2</sub>, WSe<sub>2</sub> nanosheets and their heterostructures. The assistance of H<sub>2</sub>O<sub>2</sub> paves the way for easy exfoliation of bulk MoSe<sub>2</sub> into the porous structure. The obtained nanosheets are highly suitable for HER as prerequisite of plenty of pores and irregular lateral edges. The significant improvement in edge/basal ratio is expected to enhance the active catalytic site density. The results shows that combination of porosity and heterostructures are useful in reducing the working overpotential of the material. Therefore, this work provides a reliable strategy to design low cost and high powered TMDs and selenides electrocatalyst for the promising application in HER electrocatalysis.

#### CRediT authorship contribution statement

**Rahul:** Conceptualization, Methodology, Software, Writing - review & editing. **Harpreet Singh:** Conceptualization, Methodology. **N.P. Lalla:** Data curation. **Uday Deshpande:** Data curation. **Sunil Kumar Arora:** Supervision, Visualization.

#### Declaration of Competing Interest

The authors declare that they have no known competing financial interests or personal relationships that could have appeared to influence the work reported in this paper.

#### Acknowledgements

The authors would like to acknowledge the Department of Science and Technology, India, for financial support under PURSE-II program. One of the authors Mr. Rahul acknowledges the Department of Science and Technology, India for providing funding support under the INSPIRE program (IF170759). The technical support provided by the IUAC Delhi and SAIF, Panjab University, Chandigarh is gratefully acknowledged.

#### References

- [1] J. Qian, T. Wang, B. Xia, P. Xi, D. Gao, Zn-doped MoSe<sub>2</sub> nanosheets as high-performance electrocatalysts for hydrogen evolution reaction in acid media, *Electrochim. Acta.* 296 (2019) 701–708, <https://doi.org/10.1016/j.electacta.2018.10.089>.

- [2] H.Y. He, Z. He, Q. Shen, Reduced graphene oxide/metallic MoSe<sub>2</sub>: Cu nanosheet nanostructures grown by a chemical process for highly efficient water splitting, *Mater. Res. Bull.* 111 (2019) 183–190, <https://doi.org/10.1016/j.materresbull.2018.11.009>.
- [3] S. Li, W. Zang, X. Liu, S.J. Pennycook, Z. Kou, C. Yang, C. Guan, J. Wang, Heterojunction engineering of MoSe<sub>2</sub>/MoS<sub>2</sub> with electronic modulation towards synergetic hydrogen evolution reaction and supercapacitance performance, *Chem. Eng. J.* 359 (2019) 1419–1426, <https://doi.org/10.1016/j.cej.2018.11.036>.
- [4] Y. Zhan, Z. Liu, S. Najmaei, P.M. Ajayan, J. Lou, Large-area vapor-phase growth and characterization of MoS<sub>2</sub> atomic layers on a SiO<sub>2</sub> substrate, *Small.* 8 (7) (2012) 966–971, <https://doi.org/10.1002/sml.201102654>.
- [5] J.N. Coleman, M. Lotya, A. O'Neill, S.D. Bergin, P.J. King, U. Khan, K. Young, A. Gaucher, S. De, R.J. Smith, I. V. Shvets, S.K. Arora, G. Stanton, H.-Y. Kim, K. Lee, G.T. Kim, G.S. Duesberg, T. Hallam, J.J. Boland, J.J. Wang, J.F. Donegan, J.C. Grunlan, G. Moriarty, A. Shmeliov, R.J. Nicholls, J.M. Perkins, E.M. Grieveson, K. Theuwissen, D.W. McComb, P.D. Nellist, V. Nicolosi, Two-Dimensional Nanosheets Produced by Liquid Exfoliation of Layered Materials, *Science* (80-.). 331 (2011) 568–571, <https://doi.org/10.1126/science.1194975>.
- [6] Q. Wang, D. O'Hare, Recent advances in the synthesis and application of layered double hydroxide (LDH) nanosheets, *Chem. Rev.* 112 (7) (2012) 4124–4155, <https://doi.org/10.1021/cr200434v>.
- [7] J. Benson, M. Li, S. Wang, P. Wang, P. Papakonstantinou, Electrocatalytic hydrogen evolution reaction on edges of a few layer molybdenum disulfide nanodots, *ACS Appl. Mater. Interfaces.* 7 (25) (2015) 14113–14122, <https://doi.org/10.1021/acsami.5b03399>.
- [8] X. Zhou, J. Jiang, T. Ding, J. Zhang, B. Pan, J. Zuo, Q. Yang, Fast colloidal synthesis of scalable Mo-rich hierarchical ultrathin MoSe<sub>2</sub>-nanosheets for high-performance hydrogen evolution, *Nanoscale.* 6 (19) (2014) 11046–11051, <https://doi.org/10.1039/C4NR02716G>.
- [9] D. Kong, H. Wang, J.J. Cha, M. Pasta, K.J. Koski, J. Yao, Y.i. Cui, Synthesis of MoS<sub>2</sub> and MoSe<sub>2</sub> films with vertically aligned layers, *Nano Lett.* 13 (3) (2013) 1341–1347, <https://doi.org/10.1021/nl400258t>.
- [10] J. Xie, J. Zhang, S. Li, F. Grote, X. Zhang, H. Zhang, R. Wang, Y. Lei, B. Pan, Y.i. Xie, Controllable disorder engineering in oxygen-incorporated MoS<sub>2</sub> ultrathin nanosheets for efficient hydrogen evolution, *J. Am. Chem. Soc.* 135 (47) (2013) 17881–17888, <https://doi.org/10.1021/ja408329q>.
- [11] Z. Lei, S. Xu, P. Wu, Ultra-thin and porous MoSe<sub>2</sub> nanosheets: facile preparation and enhanced electrocatalytic activity towards the hydrogen evolution reaction, *Phys. Chem. Chem. Phys.* 18 (2016) 70–74, <https://doi.org/10.1039/c5cp06483j>.
- [12] S. Zhang, J. Liu, K.H. Ruiz, R. Tu, M. Yang, Q. Li, J. Shi, H. Li, L. Zhang, T. Goto, Morphological evolution of vertically standing molybdenum disulfide nanosheets by chemical vapor deposition, *Materials (Basel).* 11 (2018), <https://doi.org/10.3390/ma11040631>.
- [13] X. Jiang, B. Sun, Y. Song, M. Dou, J. Ji, F. Wang, One-pot synthesis of MoS<sub>2</sub>/WS<sub>2</sub> ultrathin nanoflakes with vertically aligned structure on indium tin oxide as a photocathode for enhanced photo-assisted electrochemical hydrogen evolution reaction, *RSC Adv.* 7 (2017) 49309–49319, <https://doi.org/10.1039/c7ra10762e>.
- [14] Y. Zheng, Y. Jiao, L.H. Li, T. Xing, Y. Chen, M. Jaroniec, S.Z. Qiao, Toward design of synergistically active carbon-based catalysts for electrocatalytic hydrogen evolution, *ACS Nano* 8 (2014) 5290–5296, <https://doi.org/10.1021/nn501434a>.
- [15] K. Xu, F. Wang, Z. Wang, X. Zhan, Q. Wang, Z. Cheng, M. Safdar, J. He, Component-controllable WS<sub>2</sub> (1-x) Se 2x evolution reaction, *ACS Nano* 2 (2014) 8468–8476.
- [16] Y. Zhao, C. Yang, G. Mao, J. Su, G. Cheng, W. Luo, Ultrafine Rh nanoparticle decorated MoSe<sub>2</sub> nanoflowers for efficient alkaline hydrogen evolution reaction, *Inorg. Chem. Front.* 5 (2018) 2978–2984, <https://doi.org/10.1039/c8qi00874d>.
- [17] D. Vikraman, S. Hussain, K. Akbar, L. Truong, A. Kathalingam, S.H. Chun, J. Jung, H.J. Park, H.S. Kim, Improved hydrogen evolution reaction performance using MoS<sub>2</sub>-WS<sub>2</sub> heterostructures by physicochemical process, *ACS Sustain. Chem. Eng.* 6 (2018) 8400–8409, <https://doi.org/10.1021/acssuschemeng.8b00524>.
- [18] A.G. Pandolfo, A.F. Hollenkamp, Carbon properties and their role in supercapacitors, *J. Power Sources.* 157 (2006) 11–27, <https://doi.org/10.1016/j.jpowsour.2006.02.065>.